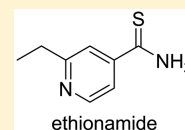


Kinetics and Mechanism of Bioactivation via S-Oxygenation of Anti-Tubercular Agent Ethionamide by Peracetic Acid

Kudzanai Chipiso,[†] Isabelle E. Logan,[†] Matthew W. Eskew,[†] Benard Omondi,[‡] and Reuben H. Simoyi^{*,†,‡}[†]Department of Chemistry, Portland State University, Portland, Oregon 97207-0751, United States[‡]School of Chemistry and Physics, University of KwaZulu-Natal, Westville Campus, Durban 4000, South Africa

ABSTRACT: The kinetics and mechanism of the oxidation of the important antitubercular agent, ethionamide, ETA (2-ethylthioisonicotinamide), by peracetic acid (PAA) have been studied. It is effectively a biphasic reaction with an initial rapid first phase of the reaction which is over in about 5 s and a second slower phase of the reaction which can run up to an hour. The first phase involves the addition of a single oxygen atom to ethionamide to form the S-oxide. The second phase involves further oxidation of the S-oxide to desulfurization of ETA to give 2-ethylisonicotinamide. In contrast to the stability of most organosulfur compounds, the S-oxide of ETA is relatively stable and can be isolated. In conditions of excess ETA, the stoichiometry of the reaction was strictly 1:1: $\text{CH}_3\text{CO}_3\text{H} + \text{Et}(\text{C}_5\text{H}_4)\text{C}(=\text{S})\text{NH}_2 \rightarrow \text{CH}_3\text{CO}_2\text{H} + \text{Et}(\text{C}_5\text{H}_4)\text{C}(=\text{NH})\text{SOH}$. In this oxidation, it was apparent that only the sulfur center was the reactive site. Though ETA was ultimately desulfurized, only the S-oxide was stable. Electrospray ionization (ESI) spectral analysis did not detect any substantial formation of the sulfinic and sulfonic acids. This suggests that cleavage of the carbon–sulfur bond occurs at the sulfinic acid stage, resulting in the formation of an unstable sulfur species that can react further to form more stable sulfur species. In this oxidation, no sulfate formation was observed. ESI spectral analysis data showed a final sulfur species in the form of a dimeric sulfur monoxide species, $\text{H}_3\text{S}_2\text{O}_2$. We derived a bimolecular rate constant for the formation of the S-oxide of $(3.08 \pm 0.72) \times 10^2 \text{ M}^{-1} \text{ s}^{-1}$. Oxidation of the S-oxide further to give 2-ethylisonicotinamide gave zero order kinetics.



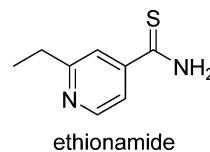
INTRODUCTION

Ethionamide, (ETA), an antimycobacterial drug is used as a second line therapeutic agent in treatment of multidrug resistant tuberculosis.¹ ETA is effective against *M. tuberculosis*, however, its use has been restricted due to its toxicity and low therapeutic index, a comparison of the amount of a therapeutic agent that causes the therapeutic effect to the amount that causes toxicity.² As a prodrug, ETA requires bioactivation to exert its pharmacological activity.³ It is oxidatively converted to its active form by the Flavin-containing monooxygenase (FMO) EtaA of *Mycobacterium tuberculosis*.⁴ This bioactivation results in reactive S-oxide intermediate,⁵ which bind to NAD^+/NADH ; forming adducts, thereby inhibiting the enoyl CoA reductase InhA.^{6,7} Mammalian flavin-containing monooxygenase (FMO) is also active toward ETA, resulting in its bioactivation.⁸

Bioactivation of drugs to reactive metabolites is an unfavorable process during drug metabolism.⁹ Precautions are always taken during drug development to eliminate possibility of reactive metabolites.^{10,11} This bioactivation appears to be the prerequisite for drug induced toxicity due to thiono-sulfur containing compounds.¹² Drugs containing a heteroatom such as sulfur, nitrogen or phosphate, which are soft nucleophiles, are easily oxygenated.¹³ S-oxygenation is crucial in metabolism of drugs containing the sulfur atom. However, the sulfur atom is bioactivated to conceivably reactive metabolites such as the S-oxide and sulfinic acid.¹⁴ Thionamides, thioureas, thiocarbamates, and thiones are S-oxygenated by FMO1 and FMO3,^{15,16} to their higher states S-oxides through sulfinic acid,¹⁷ which can react with macromolecular cellular proteins, forming protein-electrophile adducts and subsequently triggering adverse drug reactions.

Sulfinic acid is, however, unstable and disproportionate to form a stable S-oxide,¹⁸ which is also a reactive intermediate, and has the capacity to also bind to cells.

A large number of antituberculosis drugs are known to be hepatotoxic. ETA's bioactivation by the host's system has been implicated in its hepatotoxicity and gastrointestinal toxicity due to ethionamide.¹⁹ Despite great strides being made in the field of toxicology, failure of drugs due to unfavorable kinetics properties as well as unsafe toxic profiles remains a challenge. Here we report on the kinetics and mechanistic information regarding oxidation of ethionamide to aid the understanding of bioactivation of similar class of xenobiotics.

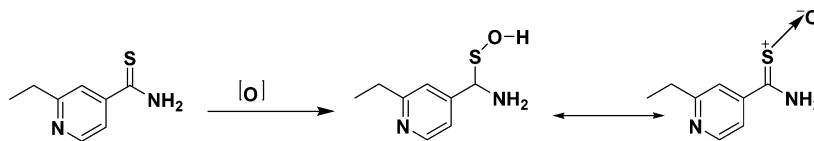


We report, in this manuscript, on the oxidation of ETA by peracetic acid. ETA bioactivation studies have been performed using liver microsomes; without a clear delineation of the products of this oxidation. Microsomes are usually nonspecific; with over 50 CYP450 genes and 15 subgenes as well as about ten Flavin-containing monooxygenases.^{20–22} Product identification after bioactivation in such environments is not trivial. Peracetic acid (and in some cases, persulfate), on the other hand, is a very “clean” oxidant; it bioactivates via oxygen addition to give acetic

Received: July 22, 2016

Revised: September 28, 2016

Scheme 1. Sulfenic Acid Formed Is Unstable with Respect to the S-Oxide



acid and an oxidized substrate; which is exactly what the confirmed ETA bioactivating monooxygenase does. Oxidation mechanisms of peracetic acid have been intensely studied and have been well-characterized. Peracetic acid oxidizes as an electrophile (as in Br_2 , HOBr , etc.). The reactivity of the peracid is determined by the electron withdrawing character of the substituents. The stronger the parent acid, the more reactive is the derived peracid. Thus, trifluoroperacetic and 2,4-dinitroperbenzoic acids are stronger oxidants than peracetic and *m*-chloroperbenzoic (MCPBA) acids. The peracetic acid we have utilized in this study is the weakest of all peracetic acids, thus ensuring a smaller subset of possible oxidation products. The vast majority of peracetic acids are used in three specific oxidations: the Baeyer–Villiger oxidation of ketones to esters, oxidation of alkenes to epoxides and oxidation of heteroatoms to their oxides: amine to amine oxides, sulfides to sulfoxides, and phosphine to phosphine oxides.^{23,24} Peracids are generally inert and do not oxidize alcohols, esters and ethers. Thus, they are the best way to mimic bioactivation of ETA by Flavin monooxygenase, EtaA,²⁵ while avoiding complicating issues associated with microsomal oxidations.

EXPERIMENTAL SECTION

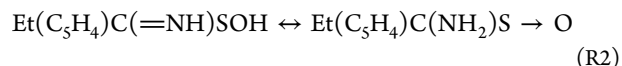
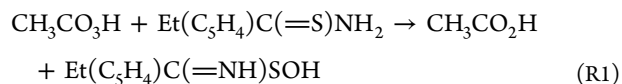
Materials. Reagent grade Ethionamide (ETA), peracetic acid, sodium chloride, perchloric acid and barium chloride were purchased from Sigma-Aldrich (USA) and were used without further purification. Water solutions for reactions were purified using a Barnstead Sybron Corp. water purification unit capable of producing both distilled and deionized water (Nanopure). Inductively coupled plasma mass spectrometry (ICPMS) was used to evaluate concentrations of metal ions in the reagent water. ICPMS results showed negligible amounts (<0.1 ppb) of copper, iron and silver ions with approximately 1.5 ppb of cadmium and 0.43 ppb in lead as the highest metal ion concentrations. In previous experiments from our lab, no discernible differences in kinetics data had been obtained between experiments run with chelators (EDTA, deferoxamine) and those run without, and so all experiments were carried out without the use of chelators.

Methods. The rapid reactions of ethionamide with peracetic acid were followed on a Hi-Tech Scientific SF61- DX2 double-mixing stopped-flow spectrophotometer. ETA and peracetic acid were in separate vessels, but both reagent vessels were maintained at the requisite ionic strength. Slower reactions involving the reactions of the S-oxide and decomposition of reaction products following oxidation of ETA were monitored on a conventional PerkinElmer Lambda 2S UV–vis spectrophotometer. All kinetics experiments were performed at 25.0 ± 0.5 °C and an ionic strength of 1.0 M (NaCl). ETA is sparingly soluble in water at neutral pH conditions, but its solubility increased in highly acidic environments. Stock solutions of ETA were prepared by first dissolving a known sample of ETA in 0.1 M perchloric acid followed by serial dilutions with water to attain the desired strength. ETA has an intense yellow color. Stoichiometric determinations were carried out by mixing various ratios of ETA and peracetic acid in tightly sealed volumetric flasks

and scanning them spectrophotometrically for depletion of ETA over periods of up to 24 h in unstirred vessels. Excess peracetic acid could be determined by adding excess acidified iodide and back-titrating with standard thiosulfate using freshly prepared starch as indicator. Mass spectra of oxidation products, were acquired on a high-resolution ($m/\Delta m = 30\,000$) Thermo Scientific LTQ-Orbitrap Discovery mass spectrometer (San Jose, CA) equipped with an electrospray ionization source. The electrospray ionization mass spectrometry (ESI-MS) source parameters were set as follows: spray voltage (kV), 2.5 in negative mode and 4.5 in positive mode; spray current (μA), 1.96; sheath gas flow rate, 20; auxiliary gas flow rate, 0.01; capillary voltage (V), –16; capillary temperature (°C), 300; and tube lens (V), –115. Detection was carried out in both the negative ionization mode and positive (–ESI). The detection parameters were set up as follows: analyzer; FTMS, positive and negative polarity; mass range; normal, resolution; 30 000, scan type; centroid.

RESULTS

Stoichiometry. The stoichiometry of this reaction was complex. Attained stoichiometry was dependent on the time of incubation as well as on the ratio of oxidant to reductant. In excess ETA of peracetic acid, a stoichiometry of 1:1 was quickly established, within 5 s, in which a single oxygen atom was inserted on to the sulfur center to form a sulfenic acid (R1) which immediately transformed into the more stable zwitterionic S-oxide (R2, see Scheme 1).



On prolonged standing, the S-Oxide formed in reaction 2 slowly decomposes to yield the final product 2-ethylisonicotinamide, which represents complete desulfurization of ETA (see Figure 1 and Scheme 2).

Figure 2 shows the ESI spectrum of a 1:1 mixture of ETA and peracetic acid before the reaction proceeds to completion. It shows a significant peak for the S-oxide as a major oxidation product. Sulfenic acids and S-oxides are difficult to stabilize in the absence of bulky groups surrounding the sulfur center. ETA is one of a few organosulfur compounds that can stabilize the sulfur center in the S(0) state when not in the polymeric S_8 state. The other major peak observed is the one for the product, 2-ethylisonicotinamide. Thus, the reaction is not discriminating enough to halt at the S-oxide, which is the equivalent of a 2-electron oxidation.

After the confirmed 1:1 stoichiometry is achieved in the first 5 s of the reaction, the second part of the stoichiometry could not be conclusively determined (see Figure 1). The most surprising aspect of this stoichiometry is the lack of sulfate production. With ionic strength maintained by NaCl, there was no other possibility of precipitation with barium chloride apart from sulfate. Figure 3 shows the ESI mass spectrum of a reaction solution in which

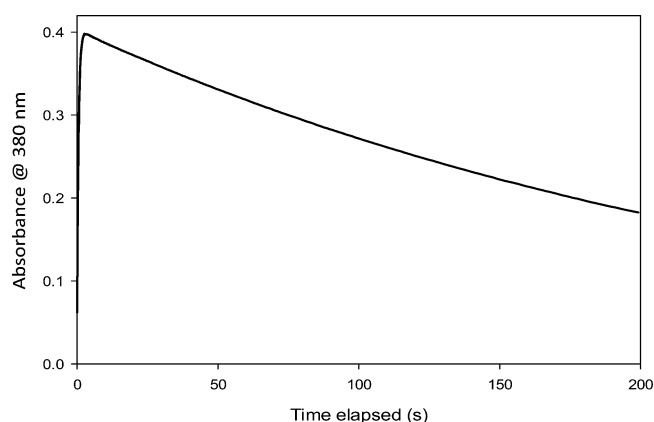


Figure 1. Absorbance trace for the reaction at 380 nm showing the biphasic nature of the reaction. The first phase of the reaction, showing formation of the S-oxide, ETAS-O, is over in 5 s. The second, slower reaction takes up to an hour for completion. This section involves further oxidation of the S-Oxide to yield the desulfurized analogue of ETA, 2-ethylisonicotinamide.

peracetic acid is in high excess over ETA, taken after prolonged standing to ensure complete consumption of ETA. The spectrum shows a single strong peak for the product, 2-ethylisonicotinamide at $m/z = 151.08682$. In a previous study, a similar compound, thionicotinamide, was oxidized by peracetic acid only as far as the sulfinic acid. Only a trace amount of the sulfinic acid of ETA is observed in this spectrum at $m/z = 191.16957$. The expected sulfate peak, even trace amounts, was not observed. Barium chloride did not afford BaSO_4 precipitation, either.

Kinetics. The kinetics of the reaction were complicated by the biphasic nature of the reaction as well as the fact that both ETA and the S-oxide absorb strongly at the wavelength of observation, 380 nm. The absorptivity coefficients of ETA and its S-oxide, ETAS-O at 380 nm are 656 and $4737 \text{ M}^{-1} \text{ s}^{-1}$ respectively. Figure 4 shows spectra of ETA and ETAS-O superimposed. Even though absorptivity of ETA is much lower than that of ETAS-O, it cannot be ignored since it is the starting material and all observed absorbance at the commencement of the reaction is derived solely from it. As the reaction proceeds, the observed increase in absorbance is due to a combination of depletion of ETA and formation of ETAS-O. An increase in absorbance is observed because the absorptivity coefficient of the product exceeds that of the reactant. Ultimately, the effective absorptivity coefficient is the difference in these two values, but to obtain unambiguous values of initial rates and rate constants for the reaction, absorbance data had to be deconvoluted and displayed with respect to each component singly and solely on its concentration variation based on Beer Law. To this effect, we are aided by the mass balance equation that says that ETA is either in its native form or in the S-Oxide form. The derivation is set up as follows:

Total concentration of ETA and ETAS-O is the initial ETA concentration, $[\text{ETA}]_0$

$$[\text{ETA}]_0 = [\text{ETA}](t) + [\text{ETAS-O}](t) \quad (1)$$

$[\text{ETA}](t)$ and $[\text{ETAS-O}](t)$ are the instantaneous concentration of ETA and the S-oxide, respectively. If we assume that ϵ_1 and ϵ_2 are the absorptivity coefficients of ETA and ETAS-O respectively, then instantaneous absorbance at any time, t is given by

$$A(t) = \epsilon_1[\text{ETA}]_0 + [\text{ETAS-O}](t)\{\epsilon_2 - \epsilon_1\} \quad (2)$$

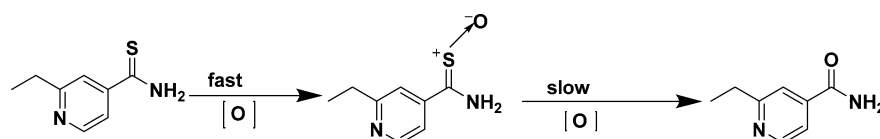
Equation 2 is correct, irrespective of whether $\epsilon_1 > \epsilon_2$ or vice versa. From eq 2, we can write a differential equation for the rate of change of absorbance with respect to time which can be qualified by the appropriate absorptivity coefficients to find rate of depletion/formation of ETA/ETAS-O. This differential equation can be integrated to evaluate the instantaneous concentrations of ETA or ETAS-O in terms of the observed overall absorbance. This gives the following analytical solution of instantaneous concentration of ETAS-O at any time with respect to the experimentally observed absorbance:

$$[\text{ETAS-O}](t) = \frac{A(t) - \epsilon_1[\text{ETA}]_0}{\epsilon_2 - \epsilon_1} \quad (3)$$

The instantaneous concentrations of ETA can thus be derived from eqs 1 and 3. The only variables in eq 3 are the concentration of ETAS-O and the observed absorbance. Since the absorbance value is known at any instantaneous time value, the corresponding concentration and absorbance can be easily derived. Each absorbance–time plot could then be deconvoluted into two separate plots; one representing the ETAS-O absorbance/concentrations, and the other ETA. Initial rates can thus be unambiguously determined. The same kinetics constants were obtained if pseudo-first-order kinetics were assumed and rate constants determined from half-lives. Figure 5 shows the multiple scans for the ETA–peracetic acid reaction. The peak at 380 nm is quickly established, and, since the scans were taken every 120 s, Figure 5 only shows the decrease of the peak at 380 nm.

Figure 6a shows the raw experimental absorbance data for the reaction while varying initial concentrations of ETA. The nonzero initial absorbance represents contribution from the initial concentrations of ETA. Using this raw experimental data would deliver an erroneously low rate of reaction and rate constant. Qualitatively, the reaction shows first order kinetics in $[\text{ETA}]_0$. The deconvoluted absorbance data, separating the absorbance contribution from ETAS-O, is obtained by applying eq 3 to every data point. This can be accomplished easily in Microsoft Excel to produce two new absorbance–time spreadsheets: one for ETAS-O and the other for ETA. Figure 6b shows the deconvoluted absorbance data derived from the ETA concentrations alone. It shows the expected decay in ETA

Scheme 2. Oxidation Scheme of ETA to Final Product^a



^aOnly the S-oxide is observed.

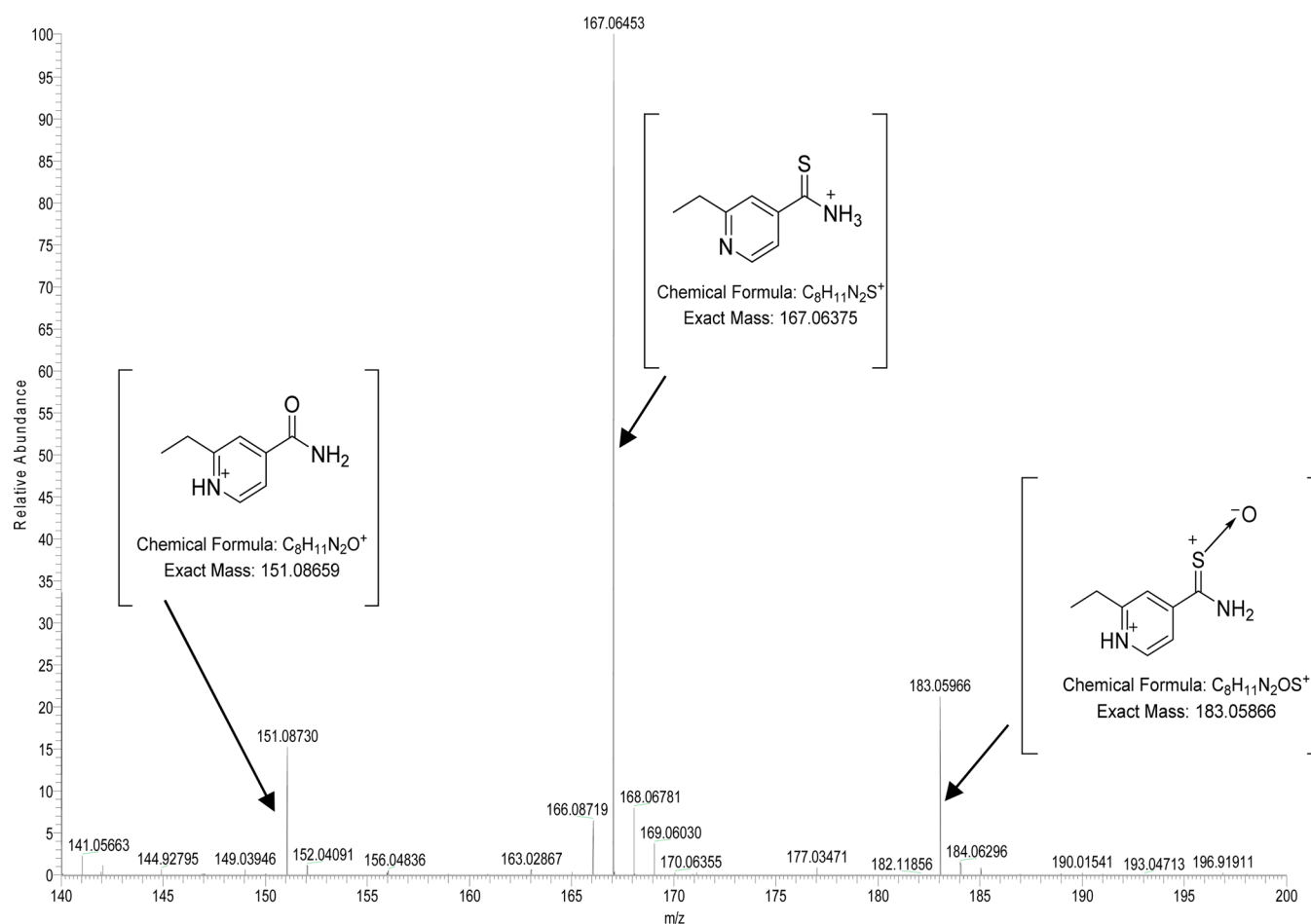


Figure 2. ESI mass spectrum of a 1:1 mixture of peracetic acid and ETA before reaction goes to full completion. It shows a strong peak for the substrate, as expected, at $m/z = 167.06389$. The S-oxide shows up at $m/z = 183.05898$. The desulfurized product, the amide, 2-ethylisonicotinamide is at $m/z = 151.08602$. No higher oxidation states of sulfur are observed.

concentrations as ETAS-O is concomitantly formed. Rate of formation of ETAS-O and rate of consumption of ETA are equivalent, based on the mass balance relation, eq 1.

In Figure 7a, peracetic acid was varied while it was still maintained in high excess over ETA. Figure 7b shows the isolation of the consumption of ETA. Again, due to the mass balance equation, these two plots mirror each other. As expected, pseudo-first order kinetics were observed. To determine reaction order with respect to peracetic acid, the variation of the observed or apparent rate constant with respect to initial peracetic acid concentration was evaluated.

$$\text{Rate} = k[\text{PAA}]^x[\text{ETA}] \quad (4)$$

We can then set $k^{\text{app}} = k[\text{PAA}]^x$, where k^{app} is the “apparent” rate constant observed. A plot of k^{app} versus $[\text{PAA}]_0$ gave a straight line. This means the order with respect to peracetic acid is 1.

We thus determined that

$$\text{Rate} = -d[\text{ETA}]/dt = k[\text{ETA}][\text{PAA}] \quad (5)$$

with $k = (3.08 \pm 0.72) \times 10^2 \text{ M}^{-1} \text{ s}^{-1}$.

Effect of Acid. Since ETA can only dissolve in an acidic environment, at any time, we never ran the reaction in higher than pH 3.0 even if no further acid was added. Figure 8 shows the inhibitory effect of acid on the reaction. One observes

a decreased rate of reaction with acid and a lower product formation.

Mechanism. The mechanism is complicated by the lack of sulfate production and the lack of any other oxidation products apart from the S-oxide. Figure 9 shows spectrum of a reaction mixture with excess oxidant and before full completion. It showed no sulfinic nor sulfonic acids, but nearly quantitative formation of the S-oxide before its slow decomposition to the amide. At this moment, only a small peak is observed for the amide.

These experimental results show that oxidation of ETA does not proceed past the S-oxide. The cleavage of the C–S bond in ETA occurs at ETAS-O. The leaving group is the radical species SO, sulfur monoxide. Concomitantly, with the extrusion of the SO moiety, is the formation of the final organic product, 2-ethylisonicotinamide. Through such well-known synthesis reactions such as the Baeyer–Villiger reaction,²³ the mechanism of peracid oxidations is well-known. The initial oxidation is an electrophilic attack by peracetic acid on the carbon–sulfur double bond. Peracids are electrophilic at the oxygen next to the acidic proton due to a strong H-bond interaction between the acidic proton and the carbonyl group of the carboxylic acid. Thus, initial oxidation of ETA involves oxygen atom addition to the nucleophilic sulfur atom via an initial epoxidation. In Scheme 3, the oxygen atom that eventually ends up on the S-oxide is the one next to the acidic proton.

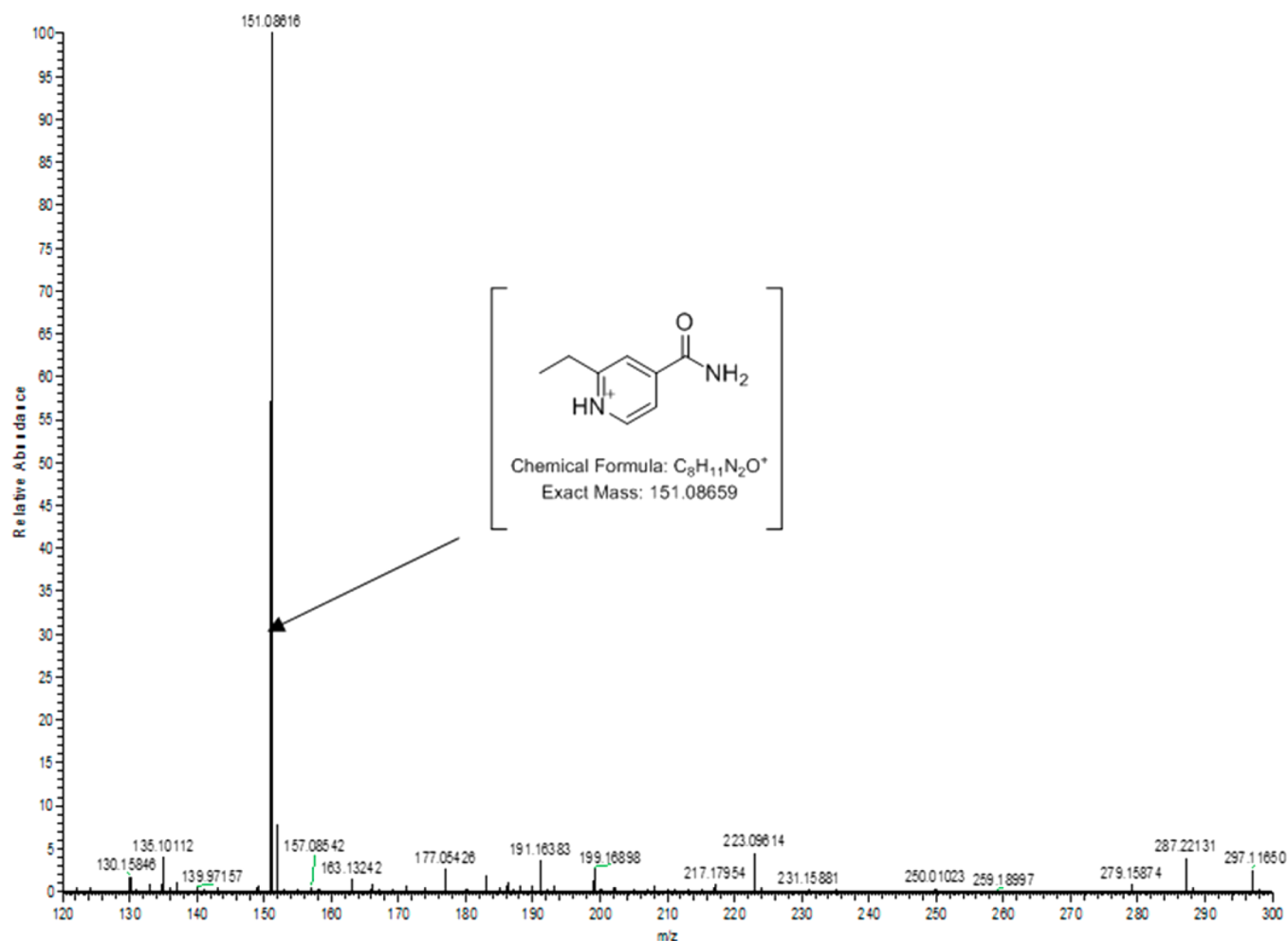
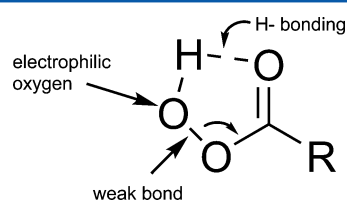


Figure 3. ESI mass spectrum obtained in high excess of peracetic acid over ETA. Only two viable peaks are observed: one for product 2-ethylisonicotinamide, and the other for the unreacted peracetic acid (not shown on this scale).



Oxidation of the thioamide bond by peracetic acid leading to the formation of the S-Oxide has been studied by our lab.²⁶ This oxidation proceeds via epoxidation and subsequent hydrolysis and rearrangement of the sulfenic acid to the S-oxide. Further research from our lab showed that the zwitterionic form of the sulfenic acid was vulnerable to cleavage of the carbon–sulfur bond, releasing a sulfoxyl anion radical that dimerizes to form dithionite.²⁷ Dithionite is distinguished by its characteristic absorbance at 315 nm as well as $m/z = 129$ ESI peak in the negative mode.

Dithionite is also easily oxidized, even by atmospheric oxygen, to sulfate. None of these dithionite spectral characteristics were observed, and, since sulfate was not observed, it appears that cleavage of the carbon sulfur bond was effected from the S-Oxide. ESI spectra were obtained which focused on m/z fragments between 60 and 120 in order to determine the final sulfur species. [Figure 10](#) shows that the major and predominant peak in this region was at $m/z = 98.95501$. Though this is close to sulfate, we were aware that it was not sulfate since no precipitate was observed with barium sulfate. This peak is attributable to the

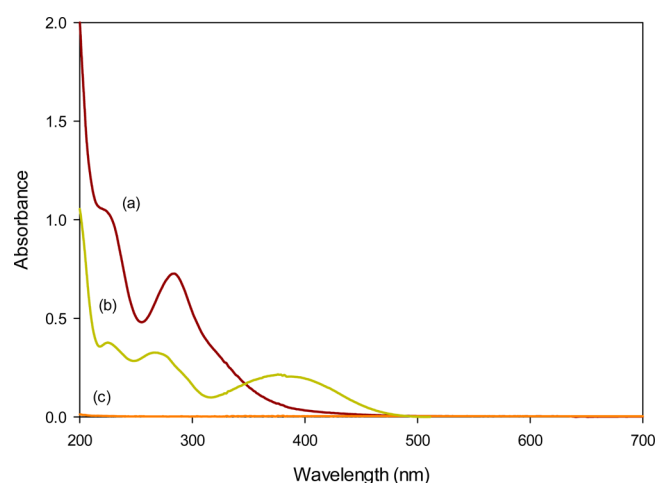


Figure 4. Spectra of (a) $[ETA] = 0.0001$ M, (b) product of $[ETA] = 0.0001$ M and per acetic acid $[PAA] = 0.00001$ M, and (c) $[PAA] = 0.0001$ M.

dimeric sulfur monoxide species, $H_2S_2O_2(aq)$. Sulfur monoxide, SO, and its dimer, S_2O_2 , have been observed in low temperatures in the gas phase.^{28,29} Sulfur monoxide has also been formed and detected in the activation of frustrated Lewis pair of N-sulfinylamine.³⁰ Thus, mechanistically, the oxidation of the

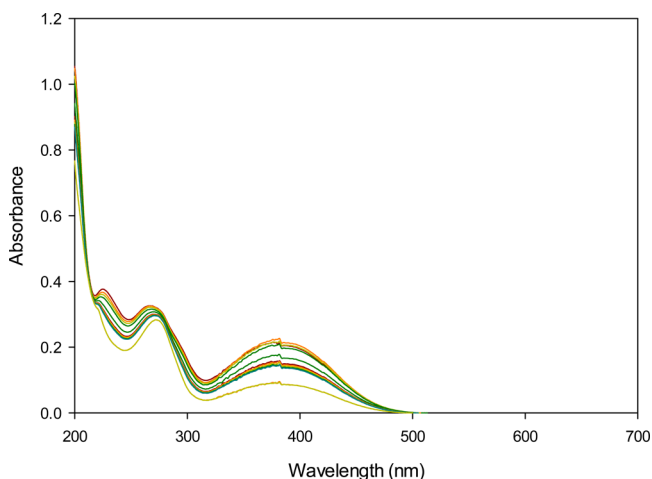


Figure 5. Multiple scan spectra showing reaction of $[ETA] = 0.0001\text{ M}$, $[PAA] = 0.005\text{ M}$. Spectra acquired every 2 min. This shows a slow decrease in the peak at 380 nm.

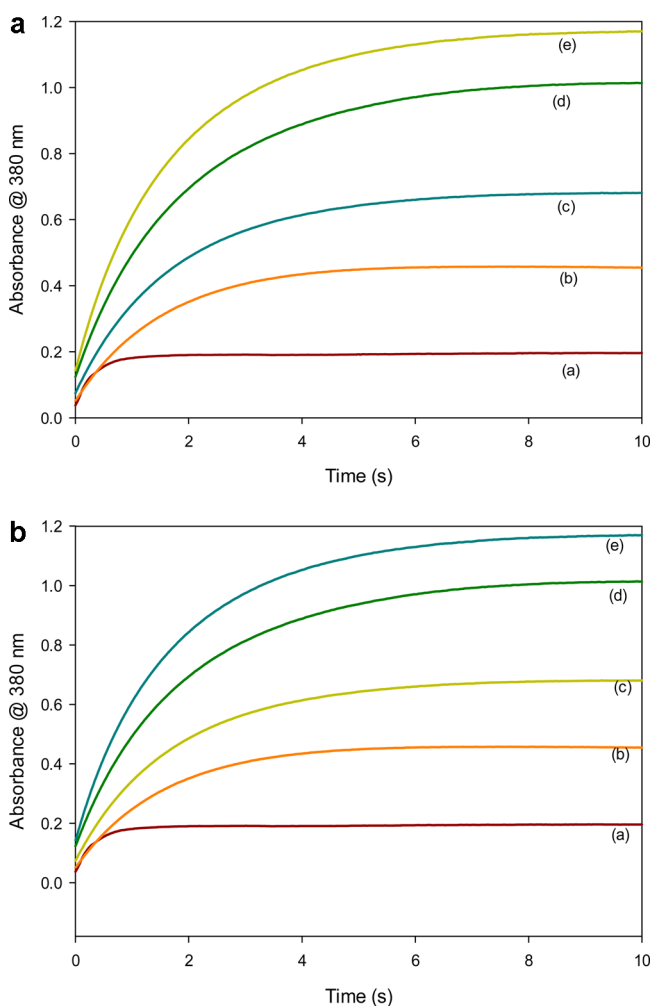


Figure 6. (a) Variation of ETA in its oxidation by per acetic acid showing total absorbance from ETA and ETAS-O at 380 nm. $[CH_3CO_3H] = 0.005\text{ M}$, $[H^+] = 0.0001\text{ M}$, $I_{NaCl} = 1.0\text{ M}$; and varied $[ETA]_0$ (a) = 0.00005 M, (b) 0.00010 M, (c) 0.00015 M, (d) 0.00020 M (e) 0.00025 M. (b) Concentration variations of ETA in its oxidation by per acetic acid showing appearance of ETAS-O at 380 nm. These traces are obtained from subtracting at each data point the absorbance in panel b from that in panel a.

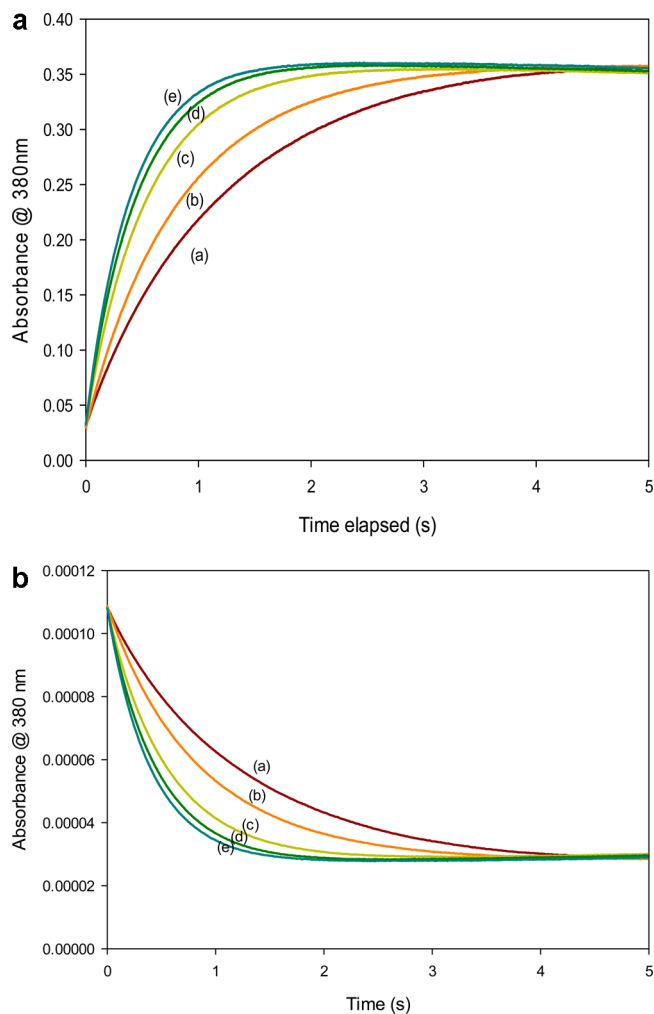


Figure 7. (a) Variation of CH_3O_3H in ETA oxidation by per acetic acid. Fixed $[ETA] = 0.0001\text{ M}$ varied $[CH_3O_3H] =$ (a) 0.00020 M, (b) 0.00030 M (c) 0.00045 M (d) 0.00055 M, (e) 0.00065 M. (b) Variation of $[CH_3O_3H]$ showing consumption of ETA. The conditions are the same as in panel a.

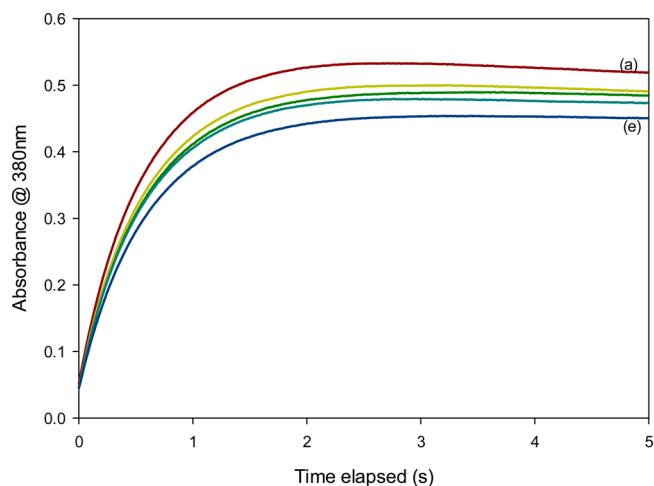


Figure 8. Variation of $[HClO_4]$. Fixed $[ETA] = 0.0001\text{ M}$, $[PAA] = 0.005\text{ M}$. Varied $[HClO_4]$ (a) 0.1 (b) 0.25 M, (c) 0.5 M, (d) 0.75 M, (e) 1.0 M. Traces a–e are sequentially from top to bottom.

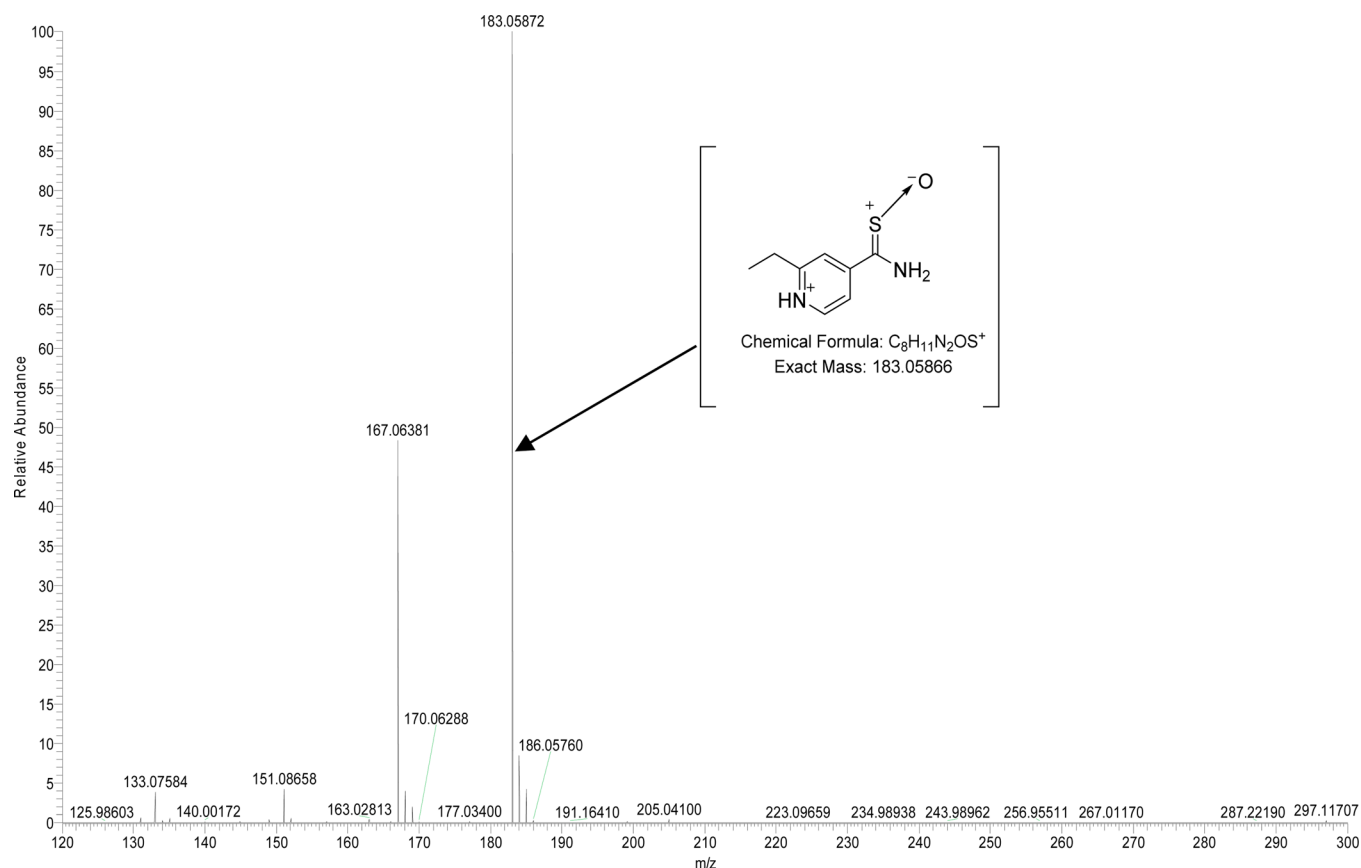
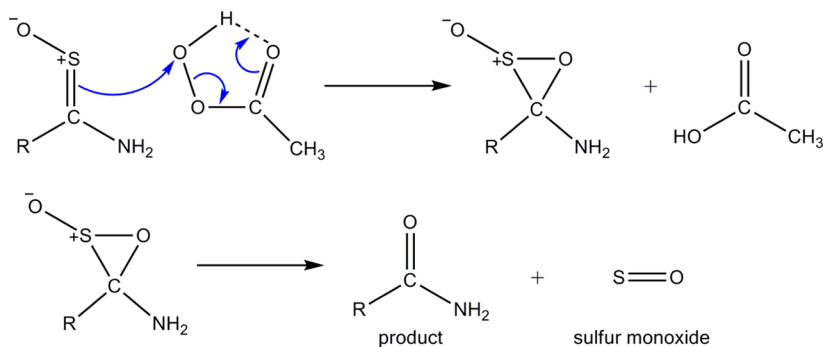


Figure 9. ESI(+) spectrum of a 1:3 mixture of ETA to peracetic acid after 5 min and before full completion of the reaction. The strongest peak is for the S-oxide and the unreacted ETA. Very little of the amide product, at $m/z = 151.08658$ is observed at this time.

Scheme 3. Further Oxidation of the S-Oxide through Epoxidation to Form the Product and Release a Reactive Leaving Species That Further Dimerizes to Give the Major Sulfur Species

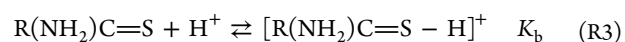


S-oxide is accompanied by the formation sulfur monoxide and the product amide (Scheme 3). Peracetic acid, a weak oxidant that oxidizes by addition of oxygen, is inert to sulfur monoxide and its dimers. Figure 10 also shows a strong peak at $m/z = 82.9541$, which is exactly 16 mass units lower than the predominant peak. This is attributable to the S_2O species which could be derived from the reaction of SO and elemental sulfur in S_6 or S_7 state before formation of the S_8 state, which is inert. Possible sulfur-based radicals, if present could be detected by EPR. Our X-Band EPR spectrometer could not detect any radical species. For these types of radicals, one needs a Q-band EPR spectrometer which was unavailable.

Scheme 3 shows the major mechanistic pathway for the oxidation of ETA. Certainly there are other minor pathways, from observation of the S_2O species. The observation of almost instant

production of the amide product without observation of a sulfenic acid indicates that formation of the product is after the formation of the S-Oxide.

Effect of Acid. Figure 8 shows the inhibitory effect of acid on this reaction. Acid reduces the rate of reaction and amount of S-Oxide formed before further desulfurization of the thioamide. The observed acid retardation occurs at very high acid conditions, at pH values between 1 and 0. At these highly acidic conditions, the thiocarbonyl group of ETA will be come appreciably protonated. The proton is known to reside between the amine and the sulfur center, but is more biased more toward the more nucleophilic sulfur center. Representing ETA as $R(NH_2)C=S$, we can then write the following equilibrium:



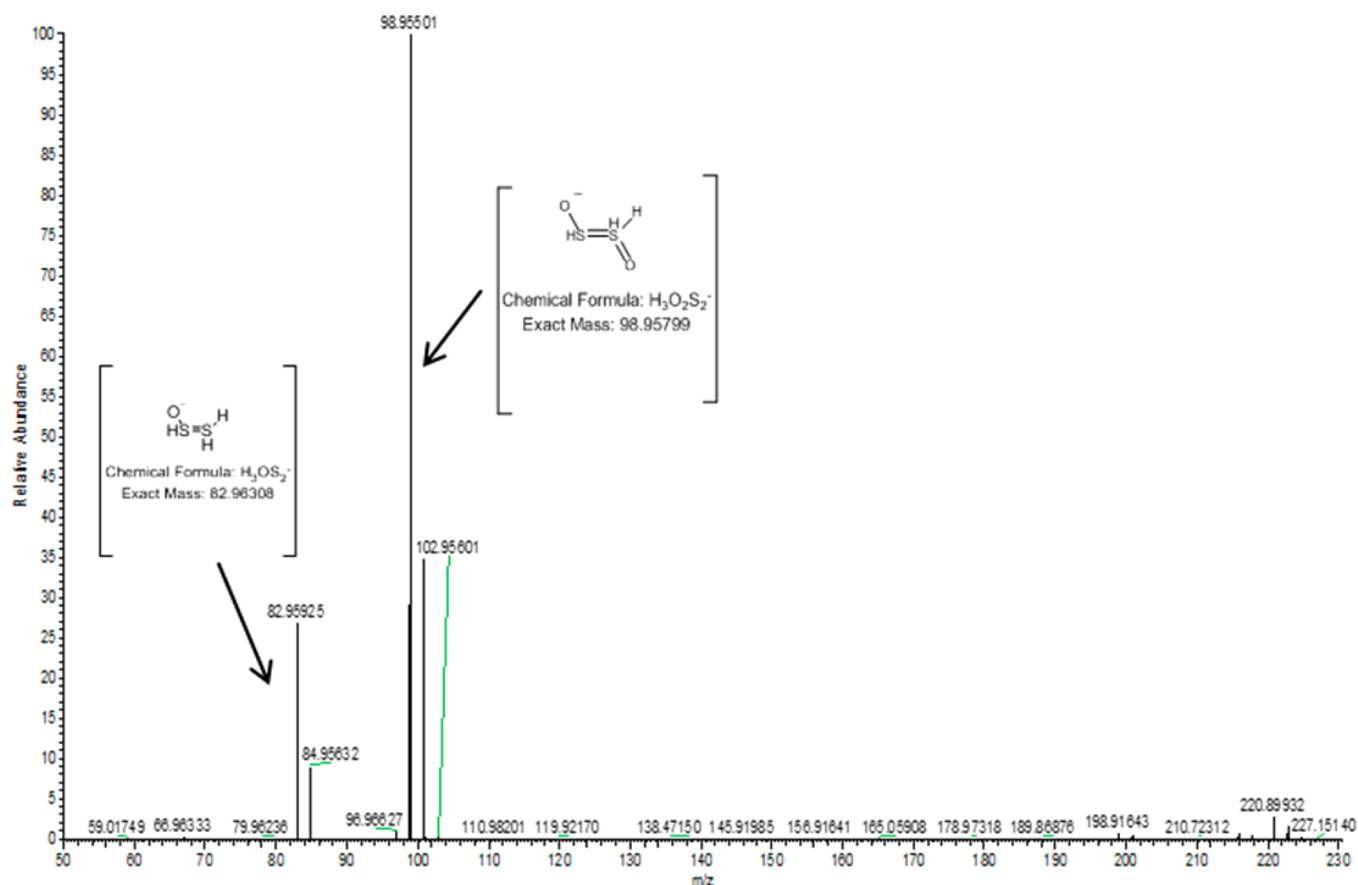


Figure 10. ESI mass spectra focusing on the sulfur species. Dimeric sulfur monoxide species is the dominant sulfur species. No sulfate was detected.

Since this is an electrophilic attack by PAA on ETA, we can consider the protonated amide to be inert, and if it does react, that this rate is exceedingly small, compared to the unprotonated thioamide. We can thus derive a more accurate rate law (eq 5) of the form

$$\text{Rate} = -d[\text{ETA}]/dt = k[\text{ETA}]_0[\text{PAA}]_0/(1 + K_b^{-1}[\text{H}^+]) \quad (6)$$

Equation 6 clearly quantifies observed acid retardation effect. The second term in the denominator is negligible at low acid concentration, and the rate reverts to eq 5. In our reaction system, acid is always present, from the PAA reactant itself, and from the initial acid amounts used to dissolve PAA. Thus, the derived rate constant represents an upper limit value in the limit very low acid concentrations.

CONCLUSIONS

This short kinetics study shows that ethionamide is oxidized by peracetic acid almost quantitatively to the S-oxide. Ethionamide, itself, is a prodrug. It is known to be metabolized to the S-oxide before interacting with its cellular target. Thus, peracetic acid can adequately mimic the microsomal bioactivation of ethionamide.

AUTHOR INFORMATION

Corresponding Author

*E-mail address: rsimoyi@pdx.edu; phone number: 503-725-3895.

Notes

The authors declare no competing financial interest.

ACKNOWLEDGMENTS

This work was funded by Grant Number CHE 1056366 from the National Science Foundation and a partial research professor vote from the University of KwaZulu-Natal.

REFERENCES

- (1) Ahmad, S.; Mokaddas, E. Recent Advances in the Diagnosis and Treatment of Multidrug-Resistant Tuberculosis. *Respiratory Medicine* **2009**, *103*, 1777–1790.
- (2) Wolff, K. A.; Nguyen, L. Strategies for Potentiation of Ethionamide and Folate Antagonists Against Mycobacterium Tuberculosis. *Expert Rev. Anti-Infect. Ther.* **2012**, *10*, 971–981.
- (3) Vannelli, T. A.; Dykman, A.; Ortiz de Montellano, P. R. The Antituberculosis Drug Ethionamide Is Activated by a Flavoprotein Monooxygenase. *J. Biol. Chem.* **2002**, *277*, 12824–12829.
- (4) Baulard, A. R.; Betts, J. C.; Engohang-Ndong, J.; Quan, S.; Mcadam, R. A.; Brennan, P. J.; Loch, C.; Besra, G. S. Activation of the Pro-Drug Ethionamide Is Regulated in Mycobacteria. *J. Biol. Chem.* **2000**, *275*, 28326–28331.
- (5) DeBarber, A. E.; Mdluli, K.; Bosman, M.; Bekker, L. G.; Barry, C. E. Ethionamide Activation and Sensitivity in Multidrug-Resistant Mycobacterium. *Proc. Natl. Acad. Sci. U. S. A.* **2000**, *97*, 9677–9682.
- (6) Nishida, C. R.; Ortiz de Montellano, P. R. Bioactivation of Antituberculosis Thioamide and Thiourea Prodrugs by Bacterial and Mammalian Flavin Monooxygenases. *Chem.-Biol. Interact.* **2011**, *192*, 21–25.
- (7) Vale, N.; Gomes, P.; Santos, H. A. Metabolism of the Antituberculosis Drug Ethionamide. *Curr. Drug Metab.* **2013**, *14*, 151–158.
- (8) Qian, L.; Ortiz de Montellano, P. R. Oxidative Activation of Thiacetazone by the Mycobacterium Tuberculosis Flavin Monoox-

ylgenase EtaA and Human FMO1 and FMO3. *Chem. Res. Toxicol.* **2006**, *19*, 443–449.

(9) Wen, B.; Fitch, W. L. Analytical Strategies for the Screening and Evaluation of Chemically Reactive Drug Metabolites. *Expert Opin. Drug Metab. Toxicol.* **2009**, *5*, 39–55.

(10) Kalgutkar, A. S.; Didiuk, M. T. Structural Alerts, Reactive Metabolites, and Protein Covalent Binding: How Reliable Are These Attributes As Predictors of Drug Toxicity? *Chem. Biodiversity* **2009**, *6*, 2115–2137.

(11) Evans, D. C.; Watt, A. P.; Nicoll-Griffith, D. A.; Baillie, T. A. Drug-Protein Adducts: An Industry Perspective on Minimizing the Potential for Drug Bioactivation in Drug Discovery and Development. *Chem. Res. Toxicol.* **2004**, *17*, 3–16.

(12) Neal, R. A.; Halpert, J. Toxicology of Thiono-Sulfur Compounds. *Annu. Rev. Pharmacol. Toxicol.* **1982**, *22*, 321–339.

(13) Cashman, J. R. Flavin-Containing Monooxygenase: The Role of Flavin-Containing Monooxygenase in Lead Design and Selection. *Encyclopedia of Drug Metabolism and Interactions* **2012**, DOI: 10.1002/9780470921920.edm010.

(14) Zuniga, F. I.; Loi, D.; Ling, K. H. J.; Tang-Liu, D. D. S. Idiosyncratic Reactions and Metabolism of Sulfur-Containing Drugs. *Expert Opin. Drug Metab. Toxicol.* **2012**, *8*, 467–485.

(15) Cashman, J. R. Human Flavin-Containing Monooxygenase: Substrate Specificity and Role in Drug Metabolism. *Curr. Drug Metab.* **2000**, *1*, 181–191.

(16) Henderson, M. C.; Siddens, L. K.; Morre, J. T.; Krueger, S. K.; Williams, D. E. Metabolism of the Anti-Tuberculosis Drug Ethionamide by Mouse and Human FMO1, FMO2 and FMO3 and Mouse and Human Lung Microsomes. *Toxicol. Appl. Pharmacol.* **2008**, *233*, 420–427.

(17) Henderson, M. C.; Siddens, L. K.; Krueger, S. K.; Stevens, J. F.; Kedzie, K.; Fang, W. K. K.; Heidelbaugh, T.; Nguyen, P.; Chow, K.; Garst, M.; et al. Flavin-Containing Monooxygenase S-Oxygenation of a Series of Thioureas and Thiones. *Toxicol. Appl. Pharmacol.* **2014**, *278*, 91–99.

(18) Chipiso, K.; Simoyi, R. H. Electrochemistry-coupled to Mass Spectrometry in Simulation of Metabolic Oxidation of Methimazole: Identification and Characterization of Metabolites. *J. Electroanal. Chem.* **2016**, *761*, 131.

(19) Ramachandran, G.; Swaminathan, S. Safety and Tolerability Profile of Second-Line Anti-Tuberculosis Medications. *Drug Saf.* **2015**, *38*, 253–269.

(20) Cashman, J. R.; Zhang, J. Human Flavin-Containing Monooxygenases. *Annu. Rev. Pharmacol. Toxicol.* **2006**, *46*, 65–100.

(21) Eswaramoorthy, S.; Bonanno, J. B.; Burley, S. K.; Swaminathan, S. Mechanism of Action of a Flavin-Containing Monooxygenase. *Proc. Natl. Acad. Sci. U. S. A.* **2006**, *103*, 9832–9837.

(22) Phillips, I. R.; Shephard, E. A. Flavin-Containing Monooxygenases: Mutations, Disease and Drug Response. *Trends Pharmacol. Sci.* **2008**, *29*, 294–301.

(23) Leipold, F.; Rudroff, F.; Mihovilovic, M. D.; Bornscheuer, U. T. The Steroid Monooxygenase From *Rhodococcus Rhodochrous*, a Versatile Biocatalyst. *Tetrahedron: Asymmetry* **2013**, *24*, 1620–1624.

(24) Berg, U.; Bladh, H.; Mpampos, K. Stereochemical Variations on the Colchicine Motif Peracid Oxidation of Thiocolchicone. Synthesis, Conformation and Inhibition of Microtubule Assembly. *Org. Biomol. Chem.* **2004**, *2*, 2125–2130.

(25) Vale, N.; Gomes, P.; Santos, H. A. Metabolism of the Antituberculosis Drug Ethionamide. *Curr. Drug Metab.* **2013**, *14*, 151–158.

(26) Olojo, R.; Simoyi, R. H. Oxyhalogen-Sulfur Chemistry: Kinetics and Mechanism of the Oxidation of Thionicotinamide by Peracetic Acid. *J. Phys. Chem. A* **2004**, *108*, 1018–1023.

(27) Aslabban, M.; Adigun, R. A.; DeBenedetti, W. J.; Mbiya, W.; Mhike, M.; Morakinyo, M. K.; Otoikhian, A. A.; Ruwona, T.; Simoyi, R. H. Detailed Mechanistic Studies into the Reactivities of Thiourea and Substituted Thiourea Oxo-Acids Part I: Decompositions and Hydrolyses of Dioxides in Basic Media. *J. Phys. Chem. A* **2014**, *118*, 11145.

(28) Mauderly, J. L.; Kracko, D.; Brower, J.; Doyle-Eisele, M.; McDonald, J. D.; Lund, A. K.; Seilkop, S. K. The National Environmental Respiratory Center (NERC) Experiment in Multi-Pollutant Air Quality Health Research: IV. Vascular Effects of Repeated Inhalation Exposure to a Mixture of Five Inorganic Gases. *Inhalation Toxicol.* **2014**, *26*, 691–696.

(29) Romero, J. V.; Smith, J. W.; Sullivan, B. M.; Mally, M. G.; Croll, L. M.; Reynolds, J. A.; Andress, C.; Simon, M.; Dahn, J. R. Gas Adsorption Properties of the Ternary ZnO/CuO/CuCl(2) Impregnated Activated Carbon System for Multigas Respirator Applications Assessed through Combinatorial Methods and Dynamic Adsorption Studies. *ACS Comb. Sci.* **2011**, *13*, 639–645.

(30) Longobardi, L. E.; Wolter, V.; Stephan, D. W. Frustrated Lewis Pair Activation of an N-Sulfinylamine: a Source of Sulfur Monoxide. *Angew. Chem., Int. Ed.* **2015**, *54*, 809–812.